



ISSN: 0067-2904

## Brain MR Images Classification for Alzheimer's Disease

Inas Ali Abdulmunem

Computer Science Department, College of Science, University of Baghdad, Baghdad, Iraq

Received: 27/11/2021

Accepted: 31/1/2022

Published: 30/6/2022

### Abstract

Alzheimer's Disease (AD) is the most prevailing type of dementia. The prevalence of AD is estimated to be around 5% after 65 years old and is staggering 30% for more than 85 years old in developed countries. AD destroys brain cells causing people to lose their memory, mental functions and ability to continue daily activities. The findings of this study are likely to aid specialists in their decision-making process by using patients' Magnetic Resonance Imaging (MRI) to distinguish patients with AD from Normal Control (NC). Performance evolution was applied to 346 Magnetic Resonance images from the Alzheimer's Neuroimaging Initiative (ADNI) collection. The Deep Belief Network (DBN) classifier was used to fulfill classification function. Weights were used to test the proposed method's recognition capacity, and the network was trained with a sample training set. As a result, this study offers a new method for identifying Alzheimer's disease utilizing automated categorization. In tests, it performed admirably With 98.46% accuracy achieved for AD and NC studied classes when combining Gray Level Co-occurrence Matrix (GLCM) features with a DBN.

**Keywords:** Alzheimer's Disease, Deep Belief Network, Gray Level Co-occurrence Matrix, Magnetic Resonance Imaging.

### تصنيف صور الدماغ بالرنين المغناطيسي لمرض الزهايمر

ايناس علي عبدالمنعم

قسم علوم الحاسوب, كلية العلوم, جامعة بغداد, بغداد, العراق

### الخلاصة

مرض الزهايمر (AD) هو أكثر أنواع الخرف انتشارًا. يُقدر معدل انتشار مرض الزهايمر بحوالي 5% بعد سن 65 عامًا وهو مرتبك بنسبة 30% لأكثر من 85 عامًا في البلدان المتقدمة. يتسبب مرض الزهايمر في تدمير خلايا الدماغ مما يؤدي إلى فقدان الأشخاص لذاكرتهم ووظائفهم العقلية والقدرة على مواصلة الأنشطة اليومية. من المحتمل أن تساعد نتائج هذه الدراسة المتخصصين في عملية اتخاذ القرار باستخدام التصوير بالرنين المغناطيسي (MRI) للتمييز بين المرضى المصابين بمرض الزهايمر والتحكم الطبيعي (NC). يتم تطبيق تطوير الأداء على 346 صورة بالرنين المغناطيسي من مجموعة مبادرة التصوير العصبي لمرض الزهايمر (ADNI). يستخدم مصنف شبكة الاعتقاد العميق (DBN) للقيام بمهمة التصنيف. تستخدم الأوزان لاختبار قدرة التعرف للطريقة المقترحة. ويتم تدريب الشبكة باستخدام عينة من مجموعة التدريب. نتيجة لذلك ،

\*Email: [inas.ali@uobaghdad.edu.iq](mailto:inas.ali@uobaghdad.edu.iq)

قدمت هذه الدراسة طريقة جديدة لتحديد مرض الزهايمر باستخدام التصنيف الآلي. أداء الطريقة المقترحة جيد في مرحلة الاختبار. تم تحقيق دقة بنسبة 98.46% للاصناف قيد الدراسة AD و NC عند الجمع بين خصائص مصفوفة التواجد المشترك ذات المستوى الرمادي (GLCM) مع مصنف DBN.

## 1. Introduction

Alois Alzheimer was the first specialist who identified the disorder as a physical disease that affects the brain and was named after him. AD is the most well-known kind of dementia. It has a collection of symptoms that include memory loss, thinking difficulties and develops when the brain is harmed by disease [1].

Alzheimer's disease is the 6<sup>th</sup> most common cause of death

in the United States, and the 5<sup>th</sup> most common cause of death among those aged 65 and up. Deaths from stroke, heart disease, and prostate cancer decreased between 2000 and 2017, whereas deaths from Alzheimer's disease increased by 145% percent [2]. Indirectly, the illness affects around 15 million relatives, companions, and guardians [3]. Computer-based Automatic Diagnosis (CAD) system seems to be an important tool for such difficult cases. In other words, it is considered to be a "double reading" system, in addition to pathological interpretation, where pathologists can take into consideration the information provided by the computer before making their final decision [4].

Therefore, automated and accurate detection of early AD offers potential assistance for effective treatment of AD [5]. Medical imaging systems play a vital role in human health care, and provides complete information about the human body for better treatment. Medical image classification can play an important part in diagnosing and teaching purposes in medicine [6]. Since CAD systems are focused on digital images, it is hoped that image analysis will help to detect AD early using MRIs to help reduce the harm caused by AD [5].

An MRI scanner uses radio waves and a high magnetic field to obtain digital images inside the brain of the tissues and architecture to spot abnormalities or cancers [7]. Contrasts in quality of the nuclear MR signal recovered from distinct brain regions can be used to improve the images. After the scanner's succession, relaxation times, T1-weighted, T2-weighted, and PD-weighted (Proton Density) (Figure 1) scans are determined and used to examine specific tissues inside the brain [8].

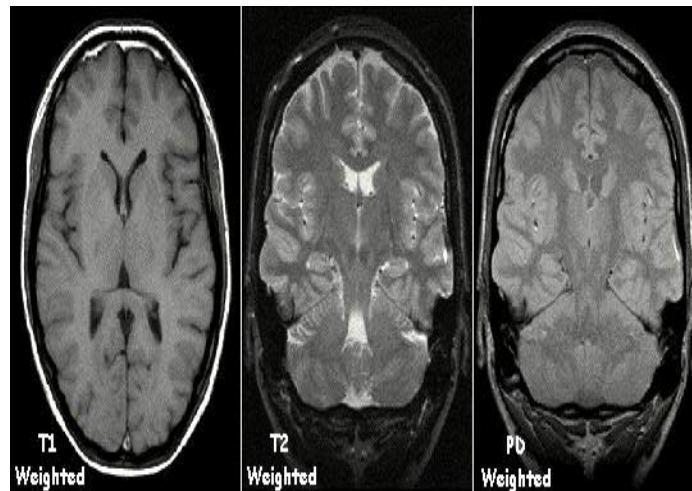


Figure 1-T1-weighted, T2-weighted and PD-weighted MRI scans Examples [9].

Neuroimaging has allowed the measurement of pathological brain changes associated with AD. Over the previous decade, these measures have been able to detect AD by using classification frameworks, which is an important tool for individualized diagnosis and prognosis [10].

## 2. Literature Review

Many studies have focused on AD detection challenges, which involves a complex set of procedures that begin with preprocessing and end with analysis, all of which are necessary to define individuals with neurodegenerative illnesses [11] When evaluating the output of the suggested methodology, gathered a dataset from the ADNI dataset. As a statistically based strategy, this research exploited an invariant moment in the feature extraction process. For classification, an Artificial Neural Network (ANN) was used. The proposed approach was found to be 94.88% accurate for AD/Mild Cognitive Impairment (MCI) and 95.58% accurate for MCI/NC.

In [12] Data from the Open Access Series of Imaging Studies (OASIS) dataset was used. They propose using an early-stage app to detect the disease. Their method necessitates: (I) The ROI is utilized to identify the areas: Hippocampus, Callosum Corpus, and Cortex; (II) the classification step is performed using SVM. They employed four different diagnostic methods: 1) Diagnosis based solely on the frontal portion (Hippocampus), 2) Diagnosis based solely on the Sagittal segment (Callosum Corpus Analysis), and 3) Diagnosis based solely on the axial section (Cortex Analysis) 4) The three sections are treated separately (Analysis of the three parts: Hippocampus, Corpus Callosum and Cortex). The fourth approach reached 90.66% compared to 73.33% for the first, 72% for the second, and 49.33% for the third. While the SVM classifier has good accuracy, its computations are expensive, and the main reason is choosing the suitable kernel function.

Subjects from the OASIS were used by [13]. Attributes were obtained from picture data as well as images that have been modified. To extract the details in this study, two types of characteristics were used. Color Mean, Symmetry, and Center Black area were calculated in the first and second groups, whereas Total Brain Area, Mean, Variance, Skewness, Image Kurtosis, Gradient Mean, and Gradient Variance were calculated in the third group. The features were used as input to both the RF classifier and the Support Vector Machine (SVM). The accuracy of the SVM classification of the OASIS-G1, OASIS-G2, OASIS-G3, and OASIS-G4 datasets was 81.58%, 86%, 73%, and 85%, respectively. The accuracy rate for RF classification of the OASIS-G1, OASIS-G2, OASIS-G3, and OASIS-G4 datasets was 84.21%, 89%, 83%, and 87%, respectively. The results of the classification show that the RF classifier outperformed the SVM classifier. The most significant disadvantage of RF is that it is far more difficult and time-consuming to construct than decision trees.

[14] used two datasets to assess the suggested method efficacy, the ADNI database and database from website of Harvard Medical School. Discrete Wavelet Transform (DWT) was utilized for features extraction, and the Principal Component Analysis (PCA) was employed to select them. Linear Discriminant Analysis (LDA) is a statistical method that has been widely used to predict class membership of observations and is used to classify NC and AD subjects. The proposed technique was evaluated with a classification accuracy of 77.78% on the ADNI dataset and 94.59% on the Harvard medical dataset.

[15] used data obtained from ADNI database. This work used five different classifiers for the predictions of the AD: SVM with accuracy of 97.56%, Gradient Boosting with accuracy 97.25%, Neural Network with accuracy of 98.36%, K-Nearest Neighbor with accuracy of 95.00%, and Random Forest (RF) with accuracy of 97.86%.

[16] used data obtained from OASIS dataset. They proposed a classification system, which is based on the results of the segmentation level set process. The viability of such a method of classification is attributed to the method of segmentation, and the field to be studied. Also, the descriptors used to extricate type to give a better result for the classification. The process comprises of considering the 4 learning samples whose entry is closest to the new X entry, by four distances: Euclidean, Manhattan, Hausdorff, Average Minimum Euclidean Distance (AMED). Foundation for estimating output of a new input X The system proved 92% accurate when detecting AD.

### 3. Materials and Methodology

#### 3.1. Materials

In agriculture applications, computer vision techniques become important due to their quick response, high precision and strong adaptability (Adaptivity refers to a system that adapts to its users automatically according to changing conditions, Adaptability applies to users who can customize the system significantly by tailoring their own activities). Two of the applications that are most pursued and widely studied relate to object detection and classification. The work is difficult due to variability in differences in product quality in some complicated natural and human-influenced circumstances [12].

Digital image processing is the method where digital images are processed using various computer algorithms. Numerous areas such as pattern recognition, image sharpening and medical image processing have been used for digital image processing [13].

The computer vision technology has different applications. Many of the most important applications are in the fields of medicine, business and security [12]. Clinical machine vision systems usually use static image processing [14]. Vision software for detecting abnormalities in medical images can be programmed. Computers can also search medical pictures and recognize possible problems far quicker than any qualified medical team [15]. Requirements for computer vision require measures such as image processing, image interpretation, and classification so that decisions based on images are feasible [12]. The medical community has many important image processing applications that often require diagnostic imaging, and it enables the medical professional to look into the human body without the need to cut it open.

Today, medical imaging is a joint project that includes physicians, physicists, engineers, and technologists. Together they can provide a standard of patient treatment that any single party operating alone would be unachievable. But in order to work together, they all need to have a solid base in medical imaging physics [17].

The ADNI is a multicenter study that aims to develop physiological, clinical, biochemical, and genetic indicators for earlier detection and surveillance of Alzheimer's disease. In 2003, Dr. Michael W. Weiner founded ADNI as an independent, privately held corporation. The main purpose of ADNI was to see if serial PET, MRI, other natural indicators, and clinical and cognitive examination could be utilized to track MCI and early AD progression. MRI, PET, genetic, clinical, and bio specimens' pictures are all included in ADNI [15]. The MRI brain pictures used in this article are from the ADNI dataset, with a focus on T1-weighted scans.

#### 3.2. Methodology

The proposed method is designed to detect the AD occurrence in the brain images from the test samples of the patients. Mainly, the established recognition system is prepared to differentiate the AD patients from NC patients.

The implemented process, like any pattern recognition program, involves two main phases: (i) Enrolment phase and (ii) Recognition phase. The method passes through three stages at each stage: (1) Pre-processing, (2) Feature Extraction, and (3) Recognition function. The block diagrams shown in Figures 2 and 3 illustrate the method stages in both phases.

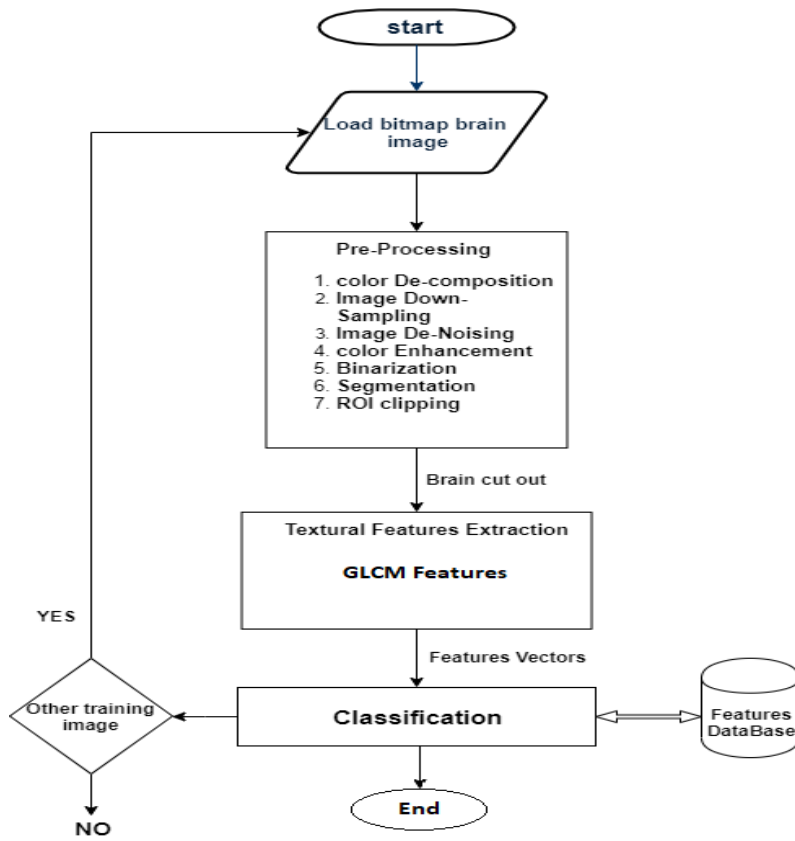


Figure 2-The layout of the proposed system (during the training phase).

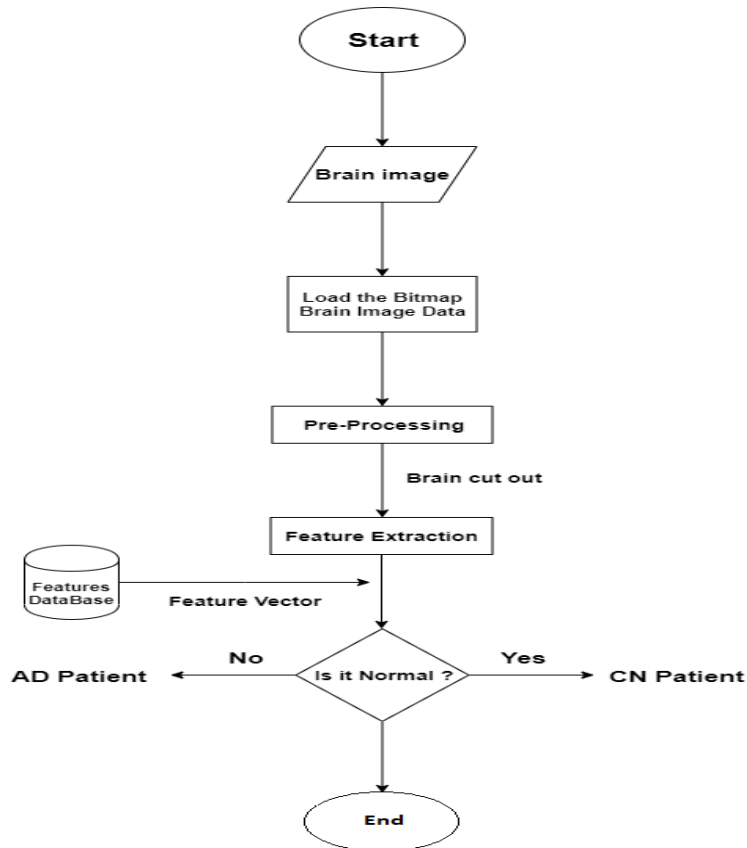


Figure 3-The layout of the proposed system (during the testing phase).

During training and recognition phase, the method passes through the following processing stages:

Stage 1: Image Loading. In this step, a PNG file of a brain image with a gray pixel resolution of 8 bit/pixel is fed into the system.

Stage 2: Preprocessing. The steps in Preprocessing are:

(i.) Color Decomposition: The loaded bitmap pixels data are fill-in the Gray array; Red (R) array is assigned to one primary color of the bitmap image. Green (G) or Blue (B) color can be used since R, G and B colors have equal values in gray images (Eq. (1)).

$$Gray = (R + G + B)/3 \quad (1)$$

(ii.) Image Down-Sampling: The images are 2048\*2048 pixels in size, and the red array has only one array so far: the red array. It is a high-resolution array, which means there are a lot of pixels to deal with, a lot of memory to store them in, and a lot of time to analyze them. As a result, this array's size must be reduced to 0.4 of its original size. Because there is no universal rule, a range of compression ratios were evaluated, ranging from 0.1 to 0.5. When the compression ratio is higher, misfortunes and artifacts are highly appeared, and the image became misshaped. As a result, 0.4 is the best value to use. The shrinking method will be bilinear sampling, which seeks to smooth out the interpolated image whether it is displayed at a size that is smaller or larger than it actually is. Interpolation between the four pixels closest to the point that best represents the new pixel produces this smoothing effect. The new pixel is given a value based on the weighted average of these four pixels. Because the future steps will deal with a smaller array of brain images, down sampling for the red array saves both time and memory space.

(iii.) Image De-Noiseing: Noise in images is treated with the use of a smoothing filter. The filter used in this study is averaging smoothing size filter (3×3). This filter depends on input image channels number. A 3×3×1 filter applied on gray-scale images (channels' number = 1). Averaging filter aims to use the pixel neighbor's mean (or average) value including itself as a substitute for the original pixel of an input image.

(iv.) Contrast Stretching Enhancement: This step is to make a contrast stretching for the gray color, so that it is stretched individually. Contrast enhancement is particularly important operation because a given image may have color intensities constrained to be within very narrow range or there the inverse situation; that is there is artificial local variation in color intensities. The unexplained color contrast differences have negative impacts on the efficiency of the system proposed. Therefore, it is important to phase contrast enhancement to make the image color data more accessible in the next stages of the developed system .

The linear stretching min-max is applied; it shifts the low color of the gray values below the defined (min) value to 0, and the high-level values above (max) are shifted to 255. The gray color level values are mapped linearly between the min and max values. As a result, the gray level range is expanded to the maximum range (0-255).

(v.) Binarization: The change from gray to black and white is completed by addition of a limit to the gray image of brain. Limit value choice is done by the user and is manually or automatically evaluated. In our built method the correct threshold value is automatically calculated. The Otsu approach is adopted; it is based on obtaining cluster-dependent image threshold value by converting a gray scale image into a binary image, which is a variable value for each image depending on the strength of the image. The threshold assessment process starts with the measurement of the number of weighted variances between two separate sets. First, we compute the histogram and probabilities of each intensity level then setting up an initial class means  $\mu_i(0)$  and the estimate of class probabilities  $\omega_i(0)$ . After that, step through all possible thresholds' maximum intensity and update  $\omega_i$  and  $\mu_i$ . Finally, calculate the intraclass variance minimization equivalent to interclass variance maximization. The optimal threshold matches the limit.

(vi.) Segmentation: The segmentation task is the major and the most difficult task in images analysis. Segmentation process is applied to partition the image into disjointed parts or objects in order to separate the brain from the skull. The image that will be segmented is the binary image. The algorithm that is used is seed filling algorithm. The Seed filling technique, which belongs to region growing type of segmentation methods, is used to divide the binary image into isolated regions based on pixels values (pixels colors), in which the set of connected pixels (4-connected region is used since a medical image has a lot of details, a 4-connected region can detect more objects than 8-connected region) with the same color and extended within bounded region is considered an isolated segment .

For example, if the start pixel is white, then it will be considered as the segment seed pixel. This seed is grown by testing its direct neighbors (along the directions: left, right, top and bottom) for white pixels. If a white pixel is met then it is added into a temporary buffer and its value in the binary image is converted to become 0 (i.e., black color). This neighbor test is done sequentially on all white pixels which are added in buffer. The scan continues until no more white pixels are added in the buffer; at this state, the contents of the buffer are considered as the isolated white segment .

After that a new seed pixel is chosen (where the seed point color is white) and the same procedure is applied to find another segment and so on until all white segments in the binary image are collected. The final result of seed filling algorithm is (N) isolated segments.

Figure 4 provides an example of a digital image and its segments after the seed filling algorithm is applied to that image. In this figure the dark cells represent the black pixels (or 0) in a binary image and light cells presents the white pixels (or 1) in that binary image, where (a) the initial binary image is before segmentation, and (b) the segments resulting from the binary image are after seed filling segmentation is applied.

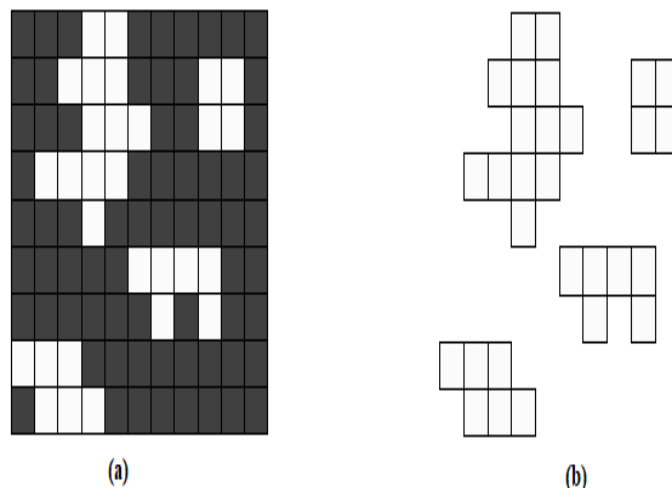


**Figure 4-**Image and its Segments: (a) A Binary Image before Applying the Seed Filling Algorithm (b) Segments of Binary Image using Seed Filling.

(vii.) ROI Extraction: This step is aimed at allocating the specific region in the brain image by maintaining the field from the original image inside the bounding ROI rectangle. The binary image from the segmentation process is the input to this point, where the brain ridges have the "one" value while the background has the "zero". To calculate the ROI in the image, each side of the image boundary is scanned until we hit the row or column.

Stage 4: Feature Extraction. After the preprocessing stage has been completed, a series of discriminating characteristics are extracted and calculated from the medical image using the information extracted from the previous stage. The features used in the proposed approach are functions of GLCM.

Texture is one of the most common tools of representation of medical images; it contributes to a wide range of image processing problems. For example, the classification of human body organ tissues using shape is difficult, but tissues are required to have clear and homogeneous texture characteristics. The texture details can therefore be used to differentiate between various tissues of organs.

Gray Level Co-occurrence Matrixes (GLCM): As mentioned earlier, the co-occurrence matrix is a frequency matrix in which the values of two pixels separated by a specified distance appear in the image. The GLCM matrix's nature is dependent on the scan direction and the distance between pixels. Since the GLCM collection of features is focused around second order statistics, changing the distance of separation allows distinct texture characteristics to be recorded, which will address valuable information on the presence and magnitude of the current local correlation between pixels. For example, two measured distances have been tested in this paper, they are (1 and 4) (in terms of homogeneity, uniformity). The spacing between pixels is one of the most important factors affecting the GLCM's capacity to discriminate. When you take distance 1, the degree of relationship between consecutive pixels (i.e., short-range neighborhood connectivity) is stated. As a result, raising the distance value implies reflecting the degree of correlation between distant pixels. It is preferable to obtain at least two sets of GLCM, one for long distance (for example, 2) and one for small distance (for example, 1), to gain a clear picture of the inter-pixel connection for the researched material (for example, 4 or higher). GLCM measured for 45°, 90° and 135° directions and all were combined in one matrix. This mixing phase aims at obtaining direction-insensitive texture features and collecting joint probabilities in all directions for more accurate performance.

After counting the frequency of each potential change between pixel values, one step remains before measurements of the texture can be determined. Normalized GLCM standardizes the co-values somewhere in the range of 0 and 1, which permits them to be seen as probabilities. Motivation of normalization is to make the features free from picture size. The Haralick features used. Also, GLCM size is quantized for faster processing:

$$I'(i, j) = (I(i, j)) / (\text{quantization value}) \quad (2)$$

The *quantization value* used in this paper is (16).

Stage 5: Classification. During the classification stage, the extracted feature pattern should be assigned to the relevant class. DBNs are commonly used in a variety of classification tasks and provides an efficient learning technique. DBNs are generative models that are trained using a Bayesian Network framed by a sequence of stacked Restricted Boltzmann Machines (RBMs). Because RBMs are used, there are no intra-layer connections (in this way the "limited" associations in Limited Boltzmann Machines). The layers also use unsupervised pre-preparing using an RBM stacking technique that combines contrastive divergence, because the execution of DBNs is heavily dependent on initialization of node [18].

The applied classification process stage was passed through two phases: (i) Training and (ii) Testing.

(i) DBN Training: The network begins with a random collection of weights in DBN training, and the training sample is introduced at the input layer. Then, the network outputs are evaluated and compared to the predicted "binary" output matrix, the error is measured, and the results are fed back from the output layer for weight adjustment. With all training collection, these steps are repeated, and the weights are changed at each time. The training continues until the stop condition is reached, the number of iterations is used as a stop condition to finish the exercise and find the network well qualified.

The number of input nodes shall be set equal to the number of the discriminating features in the defined system. The number of hidden neurons should be less than twice as high as the input layer (10, 15 used hidden layer). During the learning process, the best value of the

learning rate was also examined, and the number of output nodes was taken as 1 since we have two classes. Normalization is performed on features before the training of the DBN.

(ii) *DBN Testing*: In testing, the trained DBN was tested using the training and testing set of the extracted final feature vectors. The aim of conducted test is to assess the system performance and the optimal parameters for each case are given. The determined feature vectors, which are extracted from the training samples, are used to tune the node weights of the DBN during the training phase. The optimal set of weights is, in turn, used in the testing step to check the proposed method performance. When the image is fed to the system, its state will be recognized by firstly performing the steps of preprocessing and segmentation stages. As next step, the brain (i.e., ROIs) is extracted and then, the GLCM features are determined from the extracted ROIs. During the testing, the normalized features are feed to the trained DBN, after initializing all links connection with the weight values that were determined during the training phase. Finally, the output of the neural network is presented to the user as normal class or abnormal class.

The system is evaluated for accuracy with Eq. (3):

$$Accuracy = ((no. of Correctly Selected) * 100) / (total images) \quad (3)$$

#### 4. Experimental Results

This section discusses in detail the outcomes of the experiments, analysis and comments on achieving the goals suggested. The efficiency of the proposed methods, including pre-processing, segmentation, ROI-Extraction, features extraction, and classification, was evaluated using the accuracy measure. Thus, a progression of studies was performed utilizing ADNI dataset comprising of 364 MRI slices of 20 patients out of which 10 patients are NC and 10 patients are AD. Nonetheless, classification method was benchmarked with the most recent modern strategies used in literature.

*Image Loading Step*: At testing phase, a brain image is fed to the system. The first applied step is Bilinear resampling to decrease the size of the images where the new size is (819x819) pixels. Abnormal MRI slice shows the loss of brain mass associated with AD which is used to differentiate abnormal MRI slice from normal MRI slice as shown in Figure 5.

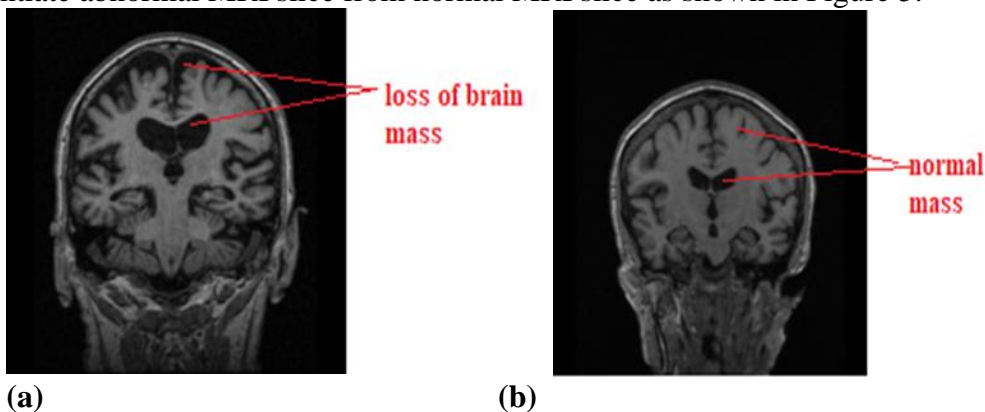


**Figure 5**-Loading abnormal and normal MRI slice. (a) Abnormal MRI slice 141 of ADNI dataset, (b) Normal MRI slice 11 of ADNI dataset.

*Preprocessing Step*: At preprocessing step, (K-mean smoothing filter, min-max contrast enhancement), is conducted as shown in Figure 6 since histogram result distribution showed the need to the preprocessing step. The preprocessing step aims to remove the background noise of the database images and improve the quality of image for the purpose of feature extraction.

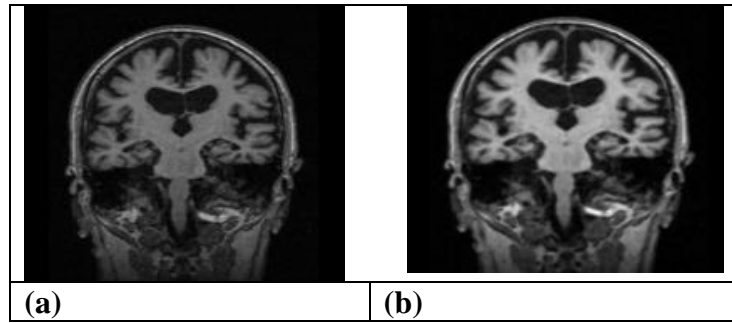


**Figure 6-** Preprocessing on MRI Slice 118 of ADNI Dataset, (a) MRI Slice before Preprocessing, (b) MRI Slice after Preprocessing.

*Binarization Step:* At the binarization stage, the Otsu [17] technique is used to conduct automatic thresholding of pictures. The algorithm returns a single intensity limit (going from 126 to 213) that partitions pixels into two groups, background and foreground, based on the picture's intensity, as illustrated in Figure 7.

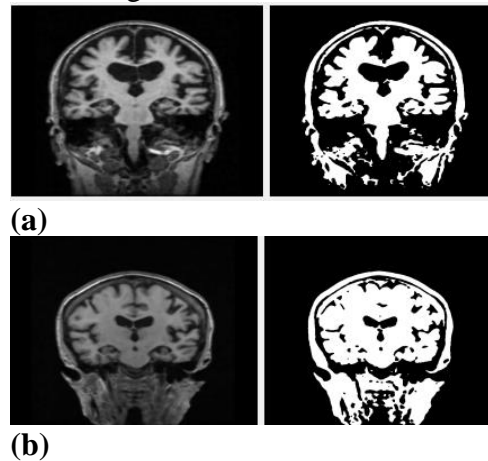


**Figure 7-** Binarization (a) Binarized Abnormal MRI Slice 118 of ADNI Dataset, (b) Binarized Normal MRI Slice 28 of ADNI Dataset.

*Segmentation Step:* the segmentation stage in this technique separated brain from skull by using a seed filling computation for determining of region associated with a node in a multidimensional array. It uses a different color to fill connected, similar-colored parts. Then, as shown in Figures 8 and 9, the array of segments is arranged in descending order to reveal the largest segment in size, which is the brain.

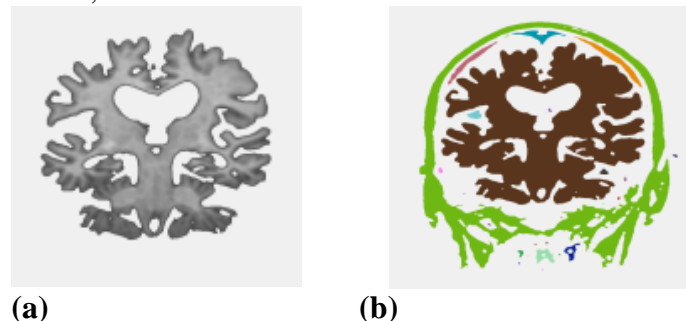


**Figure 8-** Seed Filling Algorithm on Abnormal MRI Slice 140 of ADNI Dataset. (a) Largest Segment of Seed Filling, (b) Colored image of Seed Filling.

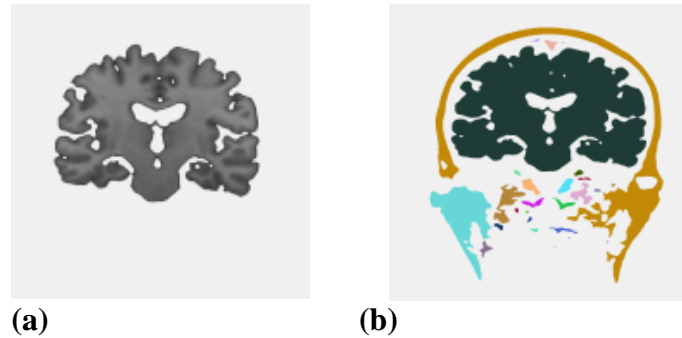


**Figure 9-** Seed Filling Algorithm on Normal MRI Slice 89 of ADNI Dataset, (a) Largest Segment of Seed Filling, (b) Colored Image of Seed Filling.

The proposed method of segmentation produced a good result. However, the proposed approach obtains a few erroneously segmented results. This indicates that the current segmentation process incorrectly captured parts of another segment and considered them to part of current segment due to pixels being connected between the two different segments as shown in Figure 10.



**Figure 10-** Mis-segmented Results of Seed Filling Algorithm. (a) Abnormal MRI Slice 173 of ADNI Dataset,(b) Normal MRI Slice 93 of ADNI Dataset.

**ROI Clipping Step:** ROI Clipping was used to boost efficiency and save time and energy by skipping pixel-related calculations that are unrelated to the calculations. Pixels that are drawn are in the brain region. Pixels that are not drawn are beyond the brain region. More informally, undrawn pixels are considered to be "clipped" as shown in Figure 11.

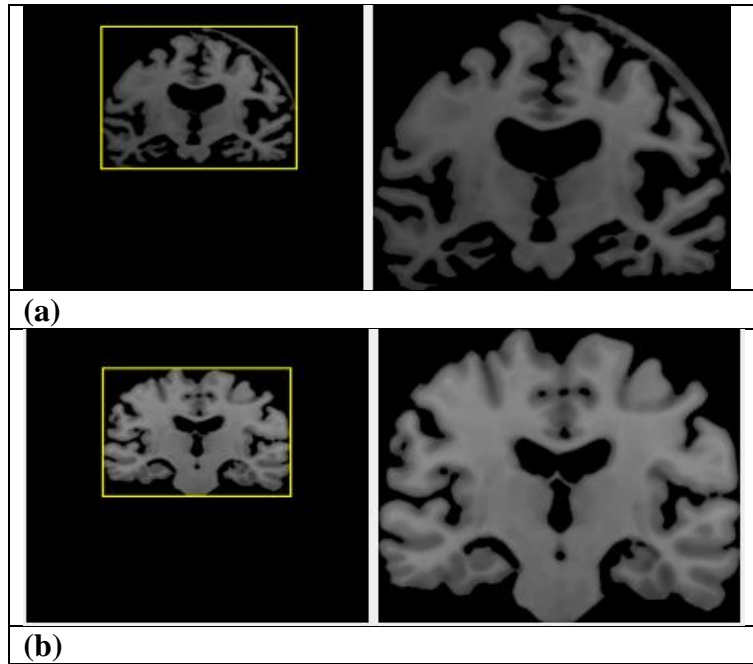


**Figure 11-** Result of ROI Clipping Step: (a) Clipped Abnormal MRI Slice 73 of ADNI Dataset,(b) Clipped Normal MRI Slice 88 of ADNI Dataset.

**Feature Extraction Step:** In the textural features extraction step, GLCM features were extracted from each image to assemble the features vector that is used to make classification for the whole taken samples (see Tables 1 and 2). There are two sets of features extracted for GLCM: one with a distance value equal to 1 and the second with distance value equal to 4.

**Table 1-**Example of GLCM Features of AD Image Slice 1 of ADNI Dataset

	Contrast	Dissimilarity	Correlation	Energy	Homogeneity
0°	339.0625	169.5781	1	1.77E+08	1526.518
45°	507.7812	252.4375	1	1.7E+08	1489.638
90°	377.4531	190.1563	1	1.75E+08	1517.299
135°	502.1562	247.7969	1	1.7E+08	1491.891

**Table 2-**Example of GLCM Features of NC Image Slice 1 of ADNI Dataset

	Contrast	Dissimilarity	Correlation	Energy	Homogeneity
0°	308.6406	163.0469	1	1.16E+08	1395.415
45°	426.4922	222.6016	1	1.11E+08	1367.54
90°	320.8672	168.2734	1	1.15E+08	1392.784
135°	456.2578	234.2266	1	1.1E+08	1363.464

As is shown by Tables 1 and 2, the features have a different value in each case depending on the angle calculated. For example, the contrast feature of NC image has a range of (308-321) when the angle is 0° and 90°, and a higher range of (426-457) when the angle is 45° and 135°, and it is the same for the AD image. This contrast in values is due to the direction of the calculation on the GLCM.

**Classification Step:** The final step is the method of classification; we used DBN to train and check the proposed framework. The accuracy levels used to assess the performance of the system are diagnosis accuracy rate, which represents the number of correctly diagnosed image samples relative to the total number of samples.

**Detection Test Based on DBN Classifier:** In this stage, a test for the two lists of features, which was acquired from feature extraction stage, was conducted to observe the discrimination power of each feature vector and to decide its suitability for recognition

purpose. The parameters of GLCM Distance (D) value, Hidden (H) layers, Learning Rate (LR) and Momentum (M) in DBN and the percentage of the training samples (MaxS) was used to test the accuracy (ACC) of the system by saving the weights of the network and then using it in the testing phase. The results of the implemented tests are given in the following sub-section

There is currently no definitive answer as to how many layers that are secret should be stacked for better results. A few hidden layers can be trained in a fairly short period of time but that would result in poor performance as the system cannot store all the features of the training datasets entirely. Too many layers can cause excessive and slow learning time. Therefore, two different settings for a number of hidden layers are checked to analyze the best case, and the results are shown in Tables 3 and 4. (Table 3 presents the DBN training parameters, and Table 4 presents the default DBN parameter values used during the training phase).

**Table 3-**The Training Parameters of the DBN

Parameter Name	Description
Number of Hidden Layers	The number of hidden layers, determined by trial and error procedure.
Range of Initial Weights	The range $[-r,r]$ of the initial weights (randomly selected);it has a significant effect on the learning speed and on the ultimate solution.
Learning Rate	The rate of gradient descent. Bigger learning rate, causes larger changes in the weights (i.e., speed up the convergence), while a small value has a complementary effect.
Momentum	It is a simple technique that often improves both training speed and accuracy.

**Table 4-**The Default Values of the DBN Parameters Used in Training Stage

Parameter Name	Description
Number of input layer	20
Number of hidden layer	15 or 10
Number of output layer	1
Range of initial weights	$[-1,+1]$

Eight cases were tested to find the best classification results of the training phase and are summarized below (Table 5 presents the best results of the 8 cases):

- 1) In the case of distance is 1, Hidden layers are 15 and using all of the training samples the best result is found when learn rate is 0.5 and the moment is 0.1 with accuracy 98.46%.
- 2) In the case of distance is 1, Hidden layers are 15 and using 75% of the training samples the best result is found when learn rate is 0.5 and the moment is 0.2, learn rate is 0.6 and the moment is 0.1 and 0.5, and when learn rate is 0.7 and the moment is 0.1 with 96.51% accuracy.
- 3) In the case of distance is 1, Hidden layers are 10 and using all of the training samples the best result is found when learn rate is 0.2 and the moment is 0.2 and when learn rate is 0.6 and the moment is 0.1 with 97.97% accuracy.
- 4) In the case of distance is 1, Hidden layers are 10 and using 75% of the training samples the best result is found when learn rate is 0.5 and the moment is 0.2 and when learn rate is 0.8 and the moment is 0.1 with 96.51% accuracy.
- 5) In the case of distance is 4, Hidden layers are 15 and using all of the training samples the best result is found when learn rate is 0.6 and the moment is 0.8 and learn rate is 0.8 and the moment is 0.9 with 97.97% accuracy.
- 6) In the case of distance is 4, Hidden layers are 15 and using 0.75% of the training samples the best result is found when learn rate is 1 and the moment is 0.2 with 96.89% accuracy.
- 7) In the case of distance is 4, Hidden layers are 10 and using all of the training samples the best result is found when learn rate is 0.7 and the moment is 0.2 with 98.26% accuracy.

8) In the case of distance is 4, Hidden layers are 10 and using 75% of the training samples the best result is found when learn rate is 0.9 and the moment is 0.1 with 96.51% accuracy.

**Table 5-**The Best Results of the 8 Cases

Case NO.	D	H	MaxS	LR	M	ACC
1	1	15	100%	0.5	0.1	98.46%
2	1	15	75%	0.5	0.2	96.51%
2	1	15	75%	0.6	0.1	96.51%
2	1	15	75%	0.6	0.5	96.51%
2	1	15	75%	0.7	0.1	96.51%
3	1	10	100%	0.2	0.2	97.97%
3	1	10	100%	0.6	0.1	97.97%
4	1	10	75%	0.5	0.2	96.51%
4	1	10	75%	0.8	0.1	96.51%
5	4	15	100%	0.6	0.8	97.97%
5	4	15	100%	0.8	0.9	97.97%
6	4	15	75%	1	0.2	96.89%.
7	4	10	100%	0.7	0.2	98.26%.
8	4	10	75%	0.9	0.1	96.51%

The time taken to train the DBN is 45 minutes and as the previous section shows the weights of DBN are adjusted for each feature using training set of dataset samples. The learning is performed first using all the dataset samples to investigate for the highest DBN classification ability. When the weights of DBN is first saved manually by writing them into a notepad file and then fed back to the system by reading the file for testing phase it did not give a correct solution due to the fact that the weights being saved and fed to system in an incorrect way and it is needed to be saved using DBN Save method so that all the network with its weights be saved and fed to the system using DBN Load method. The Save method writes the weights into a specific file but it is unreadable to the user because it appears as rubbish.

After reaching a successful training state, the trained network weights that led to the highest classification was used for AD detection, it was used as input set to the DBN in testing phase. Since there are two classes of image samples to be recognized, one output layer is taken. The tested image will go through the same steps in training phase of preprocessing, segmentation, ROI clipping, feature extraction, and finally Classification to determine which class the image belongs to as shown in Figure 12.

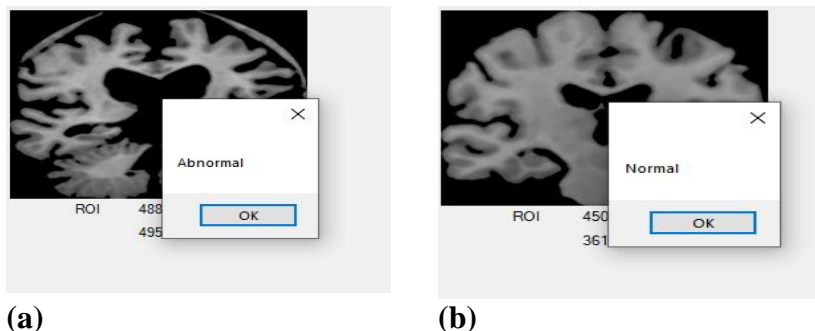


**Figure -12-** Result of Classification Step (a) Classified MRI Slice 133 of ADNI Dataset as Abnormal Case,(b) Classified MRI Slice 85 of ADNI Dataset as Normal Case.

### 5. Performance Evaluation and Comparison with Previous Studies

The proposed method of detection produced a fairly good result. However, a few wrongly classified results are obtained using the proposed process, which is also called misclassified. The term misclassified is described as "an abnormal brain MRI, but it was labeled as normal

by the system". This suggests that the current detection process wrongly identified and found the abnormal areas normal since the threshold value was similar to the normal ratio than the abnormal ratio as shown in Figure 13.

However, the performance results achieved by the proposed method for the ADNI dataset, where excellent results with 98.46% for accuracy despite the MR images difficulty. The error percentage of the system was 1.6. These results can be considered conclusive evidence of the success of the presented method to detect AD.

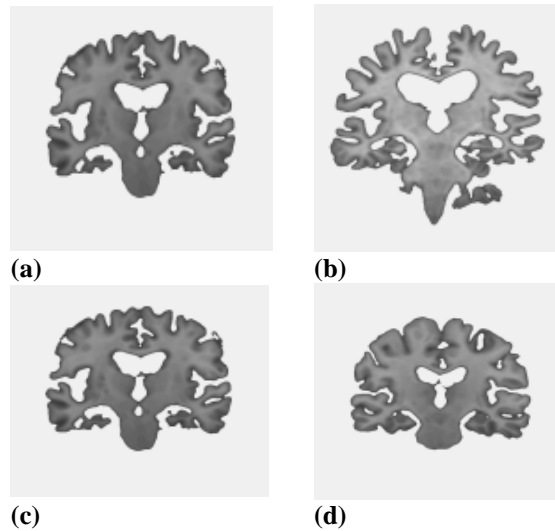


**Figure 13-** Shows the Proposed Method Misclassified the Brain MRI. (a) Misclassified Abnormal MRI Slice 162 as Normal, (b) Abnormal MRI Slice 144 of ADNI Dataset. (c) Misclassified Abnormal MRI Slice 162 as Normal, (d) Normal MRI Slice 85 of ADNI Dataset.

In recent years, a few techniques for recognizing AD have been set up, and their findings published over literature. This section makes a comparison between the proposed technique with some of the methods described in the literature.

Table 6 compares the detection accuracy accomplished by the proposed method with those gave in past studies, considering that various datasets have been utilized in these studies. The discoveries referenced show that the proposed methodology is outperforming other strategies

Although, [12] has higher accuracy, the study did not mention the features nor the number of features and the study mentioned using ADNI dataset but did not mention the number of images used.

**Table 6-**Comparison between Proposed Method with Other Methods

Study	Dataset	Method	Accuracy
Proposed method	ADNI dataset	DBN	98.46%
[13]	ADNI dataset	ANN	94.84%
[14]	ADNI dataset	LDA	77.80%
		SVM	97.56%
[14]	ADNI dataset	Gradient Boosting	97.25%
		Neural Network	98.36%
		K-Nearest Neighbour	95.00%
		RF	97.86%

## 6. Conclusion

This study included all the experimental findings that led to the proposed technique. The ADNI standard dataset was used to guide a series of experiments. For the characterization of MRI slices, the proposed approach was used. The outcomes of the experiment are researched,

decrypted, considered, approved, benchmarked, and assessed. The final results are extremely positive and unquestionably the finest. Aside from presenting exploratory results, numerous investigations and discussions on the results were also presented. The proposed methods' strengths and weaknesses were also discussed. Finally, several existing strategies available in the literature were examined in depth to confirm the suggested method's dependence. The suggested technique is designed to be far more effective than current efforts in this area.

## Reference

- [1] David Henry Small, R. Cappai., "Alois Alzheimer and Alzheimer's Disease: A Centennial Perspective," *J. Neurochem*, vol. 99, no. 3, p. 708–710, 2006.
- [2] Alzheimer Association, "Alzheimer's Disease Facts and Figures," *Alzheimer's & dementia*, vol. 15, no. 3, p. 321–387, 2019.
- [3] Bondi, M.W., Edmonds, E.C. and Salmon, "D.P. Alzheimer's disease: Past, Present, and Future," *Journal of the International Neuropsychological Society*, vol. 23, no. 9-10, pp. 818-831, 2017.
- [4] K. Doi, "Computer-aided diagnosis in medical imaging: Historical review, current status and future potential," *Computerized Medical Imaging and Graphics*, vol. 31, no. 4-5, p. 198–211, 2007.
- [5] Mohamed M. Dessouky, et al, "Computer-Aided Diagnosis System for Alzheimer ' s Disease Using Different Discrete Transform Techniques," *American Journal of Alzheimer's Disease & Other Dementias*, vol. 31, no. 3, pp. 282-93, 2015.
- [6] Heba Kh. Abbas, et al, "Analytical Study of Medical Image Combination Techniques," *Iraqi Journal of Science*, vol. 59, no. 3B, pp. 1538-1547, 2018.
- [7] Mohammed S. H. Al-Tamimi, Ghazali Sulong, "Tumor Brain Detection through MR Images: A Review of Literature," *Journal of Theoretical and Applied Information Technology*, vol. 62, no. 2, pp. 378-403, 2014.
- [8] Mohammed S. H. Al-Tamimi, and Ghazali Sulong, "A Review of Snake Models in Medical MR Image Segmentation," *Jurnal Teknologi*, vol. 2, p. 101–106, 2014.
- [9] D. A. Pollacco, "Magnetic Resonance Imaging," *BSc Maths and Physics University of Malta*, 2017.
- [10] Saima Rathore, et al, "A review on neuroimaging-based classification studies and associated feature extraction methods for Alzheimer's disease and its prodromal stages," *Neuroimage*, vol. 155, p. 530–548, 2017.
- [11] Gorji HT , Haddadnia J, "A novel method for early diagnosis of Alzheimer's disease based on pseudo Zernike moment from structural MRI," *Neuroscience*, vol. 305, p. 361–371, 2015.
- [12] Amira Ben Rabeh, Faouzi Benzarti, Hamid Amiri, "Diagnosis of Alzheimer Diseases in Early Step Using SVM (Support Vector Machine)," *2016 13th International Conference on Computer Graphics, Imaging and Visualization (CGiV)*, p. 364–367, 2016.
- [13] D. Selvathi , T. Emala, "MRI brain pattern analysis for detection of Alzheimer's disease using random forest classifier," *Intell. Decis. Technol*, vol. 10, no. 4, p. 331–340, 2016.
- [14] Heba Mohsen , et al., "Classification of Brain MRI for Alzheimer ' s Disease Based on Linear Discriminate Analysis," *Egyptian Computer Science Journal*, vol. 41, no. 3, pp. 44-52, 2017.
- [15] Priyanka Lodha, Ajay Talele, Kishori Degaonkar, "Diagnosis of Alzheimer's Disease Using Machine Learning," *Proc. - 2018 4th Int. Conf. Comput. Commun. Control Autom. ICCUBEA 2018*, p. 1–4, 2018.
- [16] Amira Ben Rabeh, Faouzi Benzarti, Hamid Amiri, "New method of classification to detect Alzheimer disease," *Proc. - 2017 14th Int. Conf. Comput. Graph. Imaging Vis. CGiV*, p. 111–116, 2018.
- [17] O. N., "A threshold selection method from gray-level histograms," *IEEE Transactions on Systems, Man, and Cybernetics*, vol. 9, no. 1, pp. 62-66, 1979.
- [18] Z. N. Shahweli, "Deep Belief Network for Predicting the Predisposition to Lung Cancer in TP53 Gene," *Iraqi Journal of Science*, vol. 61, no. 1, pp. 171-177, 2020.